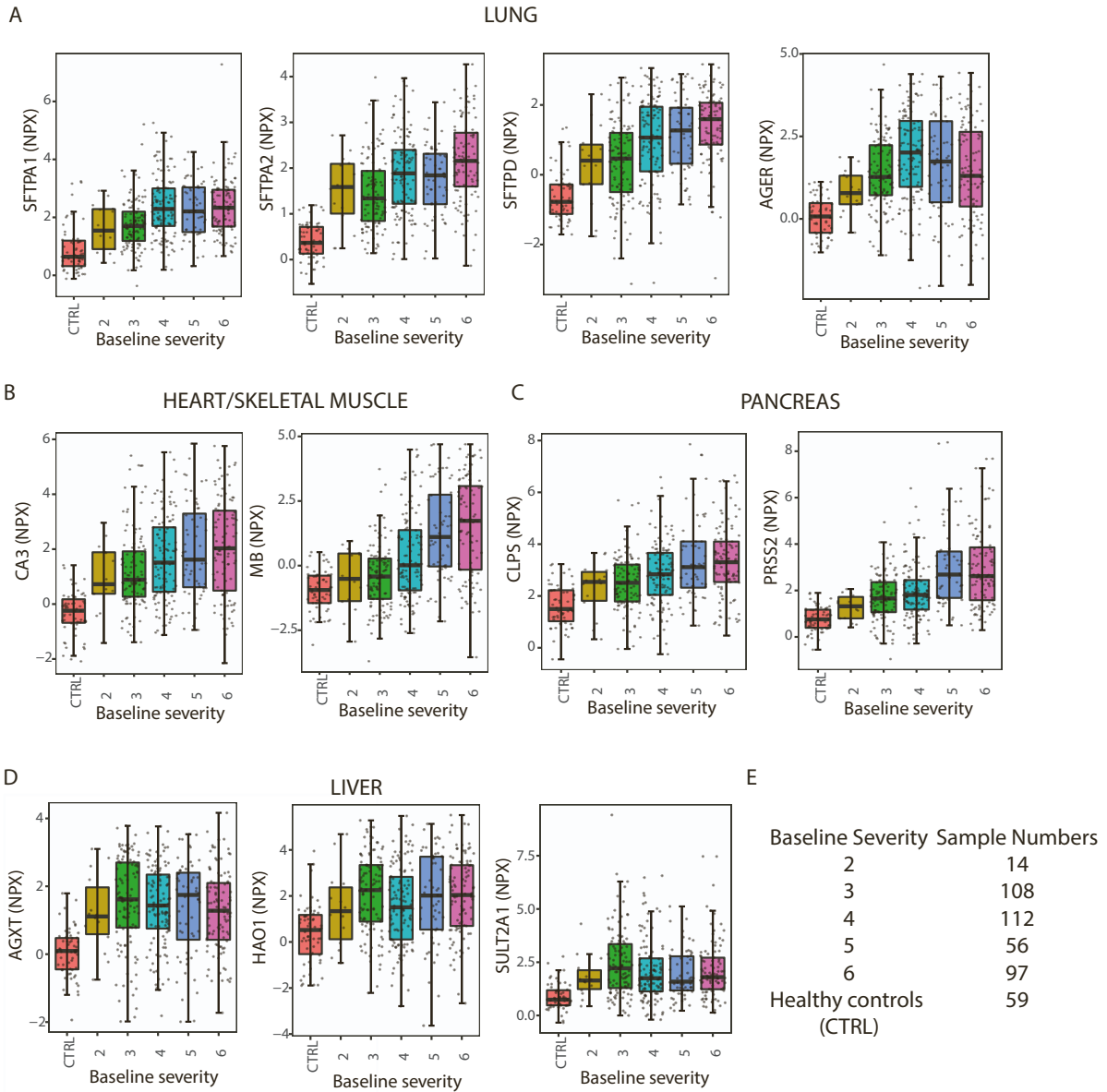


**Supplemental information**

**Transcriptomic and proteomic assessment  
of tocilizumab response in a randomized controlled  
trial of patients hospitalized with COVID-19**

**Haridha Shivram, Jason A. Hackney, Carrie M. Rosenberger, Anastasia Teterina, Aditi Qamra, Olusegun Onabajo, Jacqueline McBride, Fang Cai, Min Bao, Larry Tsai, Aviv Regev, Ivan O. Rosas, and Rebecca N. Bauer**

**Supplementary materials:**



**Figure S1. Related to Figure 2. Severity-associated changes in serum levels of organ-specific proteins.** Boxplots showing changes in serum levels across baseline severity scores for (A) lung-, (B) heart-/skeletal muscle-, (C) pancreas-, and (D) liver-specific proteins. Number of patient samples analyzed is indicated in the table (E).

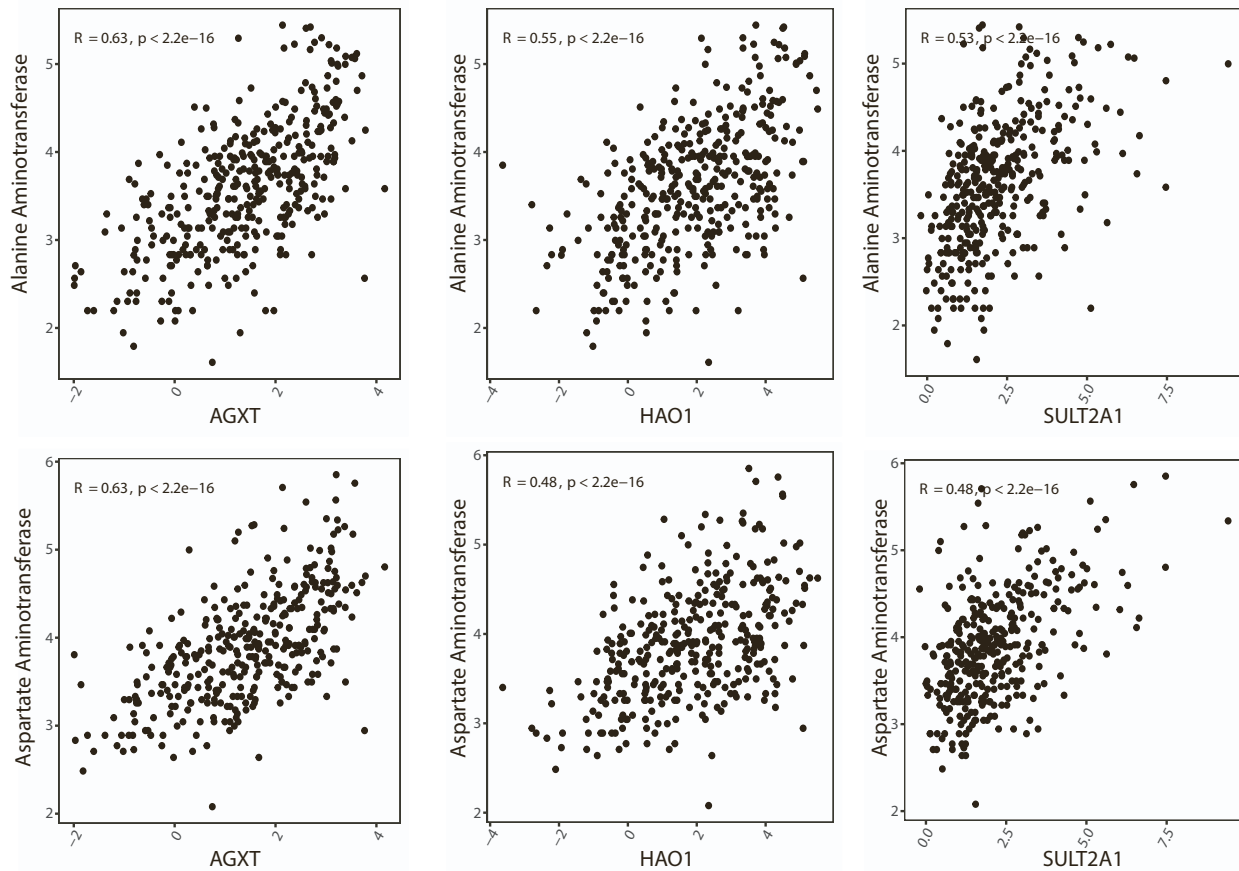


**Figure S2. Related to Figure 2. Association of liver-specific proteins to clinical biomarkers indicative of liver dysfunction.** Scatter plot comparing Olink measurements of liver-specific proteins (X-axis) to liver function test results (Y-axis) – alanine transaminase (top) and aspartate transaminase (bottom).

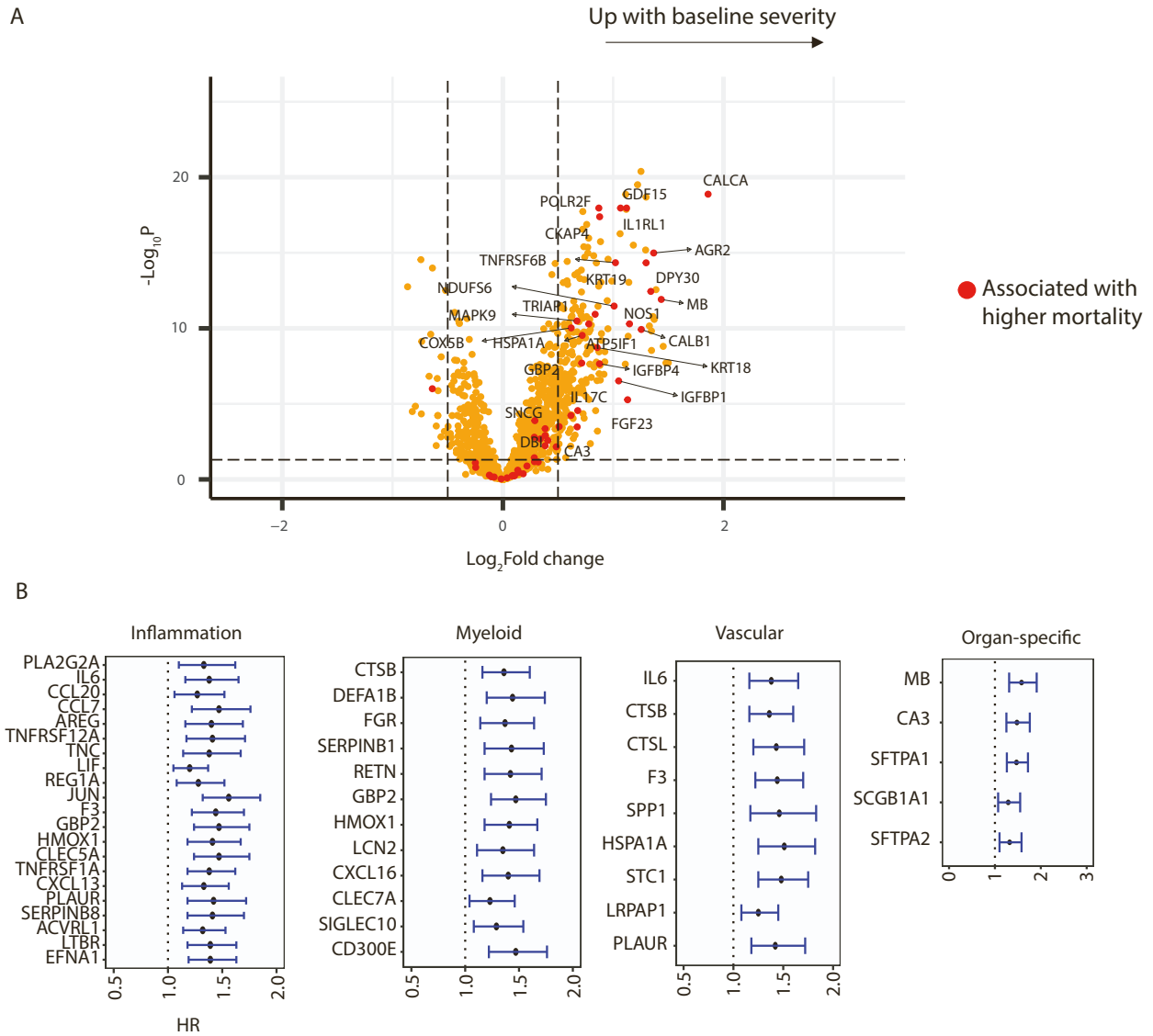


**Figure S3. Related to Figure 2. Proteins prognostic for higher mortality and clinical failure. (A)**

Volcano plots showing proteins differentially regulated in severe COVID19 as determined by Olink.

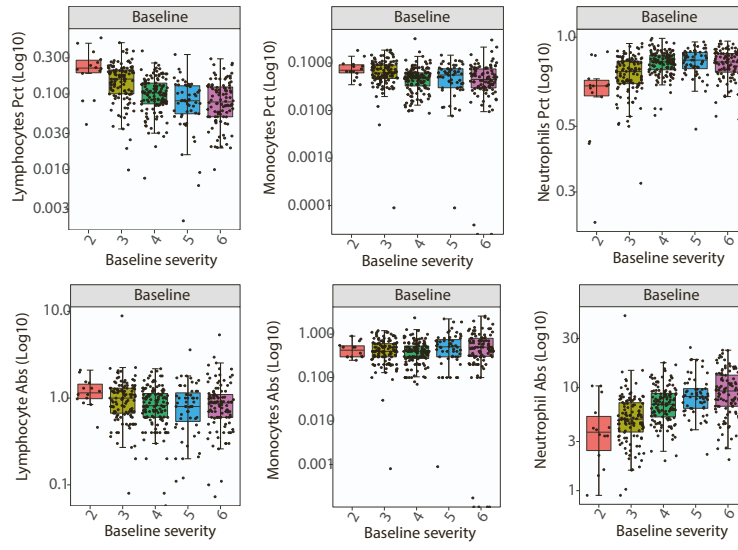
Proteins highlighted represent those that are significantly upregulated by at least +0.5 log<sub>2</sub>fold in

nonsurvivors by day 28. **(B)** Proteins prognostic for worse clinical outcome (time to clinical failure)

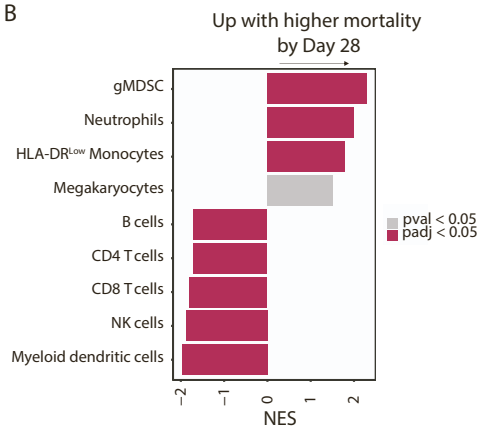
identified using Cox proportional hazard model. Only proteins showing statistically significant prognostic association are shown (Benjamini-Hochberg adjusted *P* value < 0.05, represented by \*\*\*).

HR, hazard ratio.

A



B



C

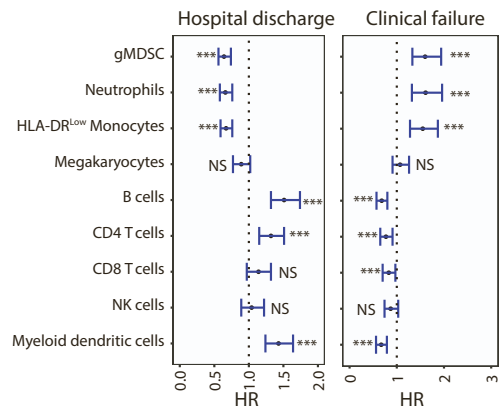


**Figure S4. Related to Figure 3. Changes in blood cell counts and biological pathways in severe COVID19 cases. (A)** Boxplots showing changes of blood cell counts with baseline severity. Percentages were calculated as ratio of specified cell type to leukocyte counts. The normal range upper limit of the absolute counts can range from 2.4-5.2  $10^9/L$  for lymphocytes, 0.36-1.5  $10^9/L$  for monocytes, and 4.8-8.89  $10^9/L$  for neutrophils. The normal range lower limit can range from 0.5-1.5  $10^9/L$  for lymphocytes, 0-0.5  $10^9/L$  for monocytes, and 0.95-3.15  $10^9/L$  for neutrophils. **(B)** FGSEA analysis of differentially expressed genes between cases associated with higher mortality (death by day 28,  $n = 83$ ) and survivors ( $n = 321$ ). Higher NES represents upregulation of the indicated immune pathway. **(C)** Forest plot showing HRs with 95% confidence intervals identified using Cox proportional hazard model depicting recovery (left) and clinical failure (right) from COVID19 for cell types shown in Figure 3D. \*\*\*Represents Benjamini-Hochberg adjusted  $P$  value  $< 0.05$ .

Abs, absolute; CD, cluster of differentiation; gMDSC; granulocytic myeloid-derived suppressor cells; HLA, human leukocyte antigen; HR, hazard ratio; NES, normalized enrichment score; NK, natural killer; NS, not significant; Pct, percent; pval,  $P$  value; padj, adjusted  $P$  value.

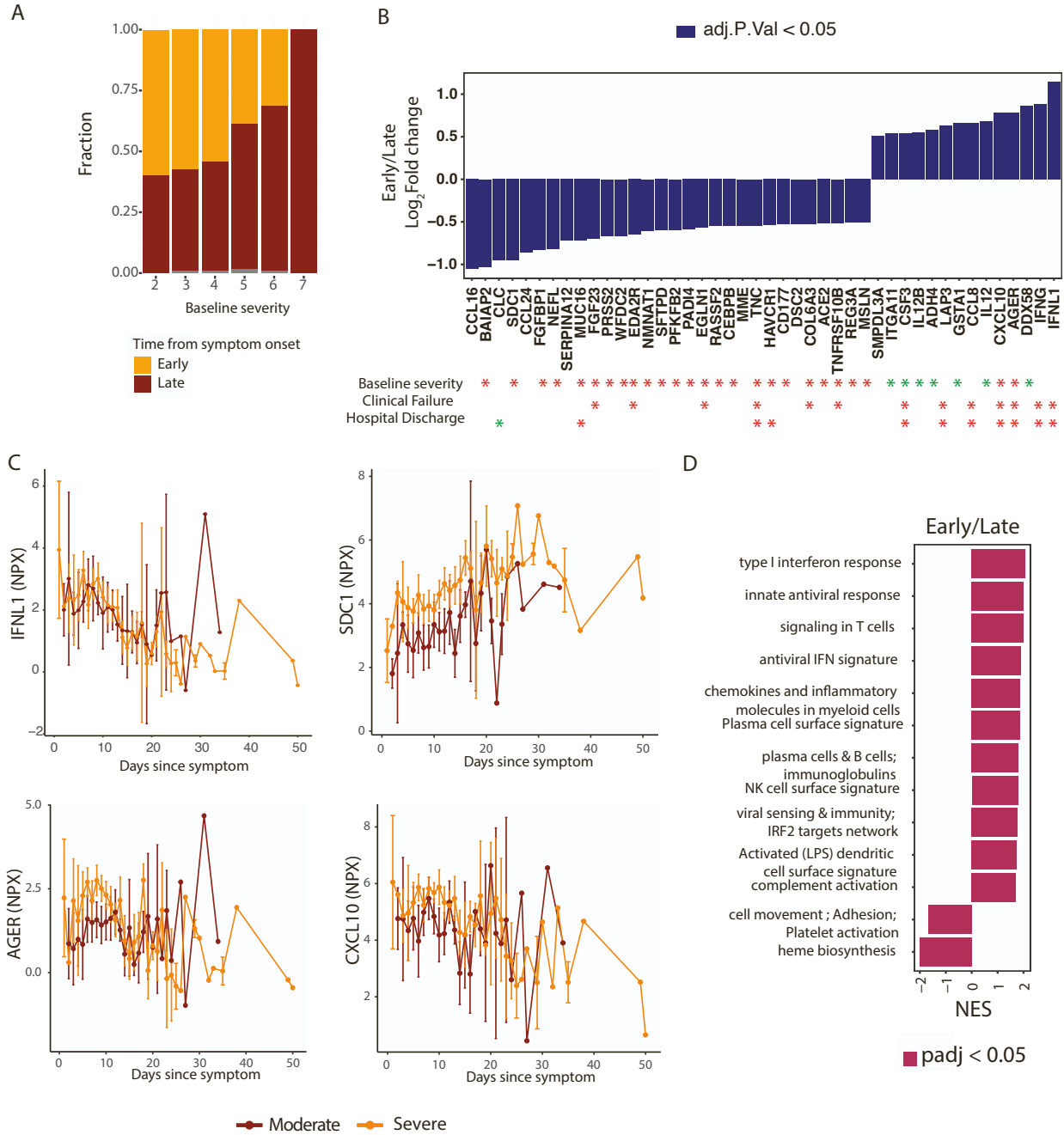


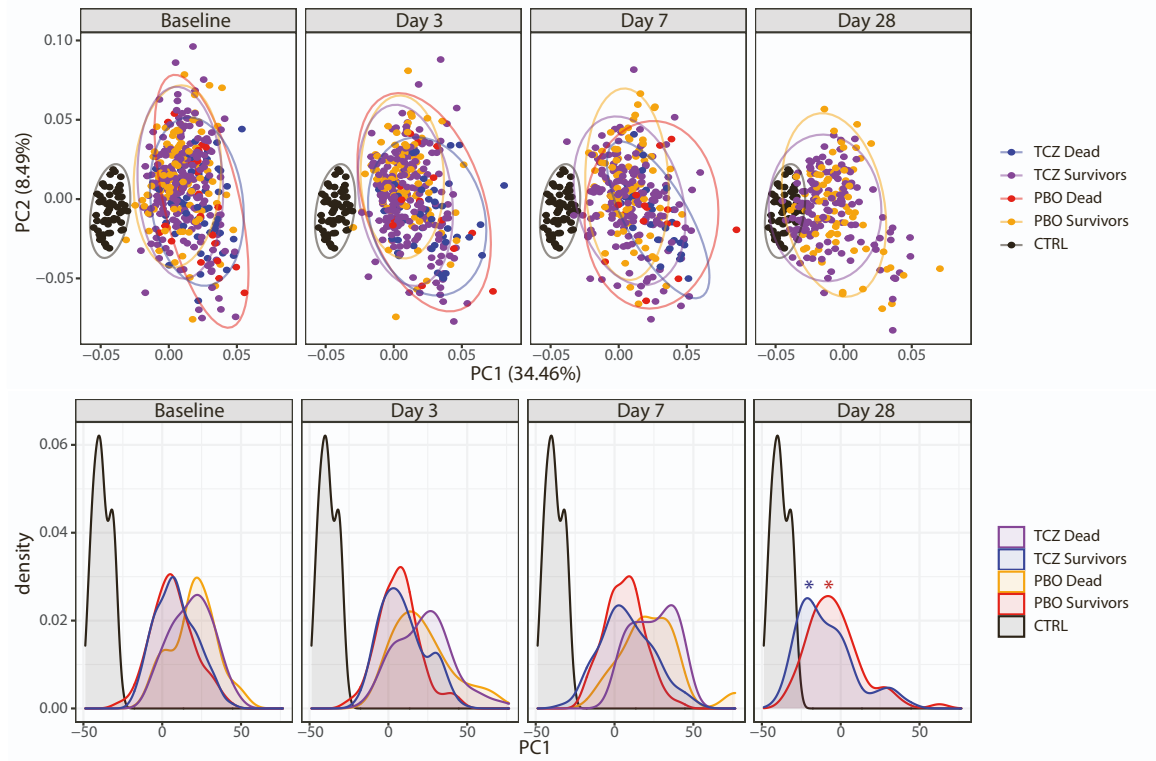
**Figure S5. Related to Figure 2 and 3. Time to symptom onset – dependent changes in protein and transcript levels at baseline. (A)** Column plot showing fraction of samples per baseline severity score sampled within 10 days of symptom onset vs later. **(B)** Column plot showing log<sub>2</sub>fold difference in the abundance (Y-axis) for the serum proteins significantly different between COVID-19 subjects sampled within 10 days (n = 182) of symptom onset vs later (n = 202). **(C)** Line plot showing baseline serum

levels of specified proteins on Y-axis and time from symptom onset of the corresponding patients. Error bars represent 95% confidence intervals around the mean. **(D)** Bar plot showing FGSEA results for immune pathways enriched among genes differentially expressed between COVID19 subjects sampled within 10 days from symptom onset (early, n = 186) vs greater than 10 days of from symptom onset (late, n = 214).

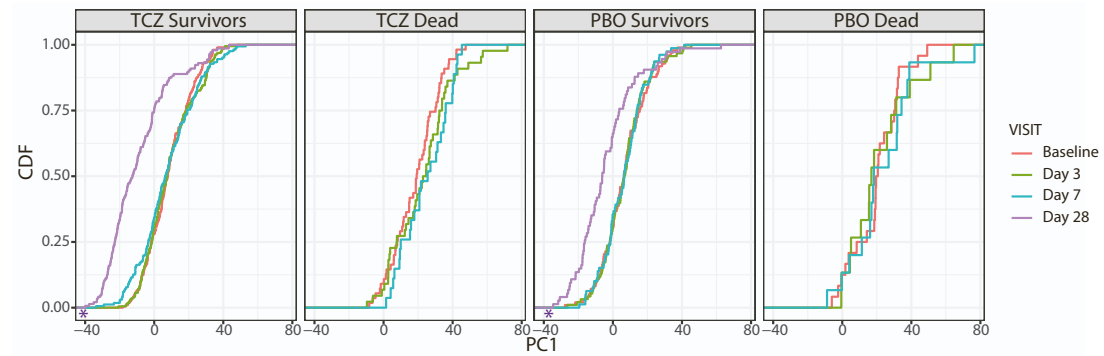
IFN, interferon; LPS, lipopolysaccharide; NES, normalized enrichment score; NK, natural killer; NPX, normalized protein expression; padj, adjusted *P* value.



A



B



C

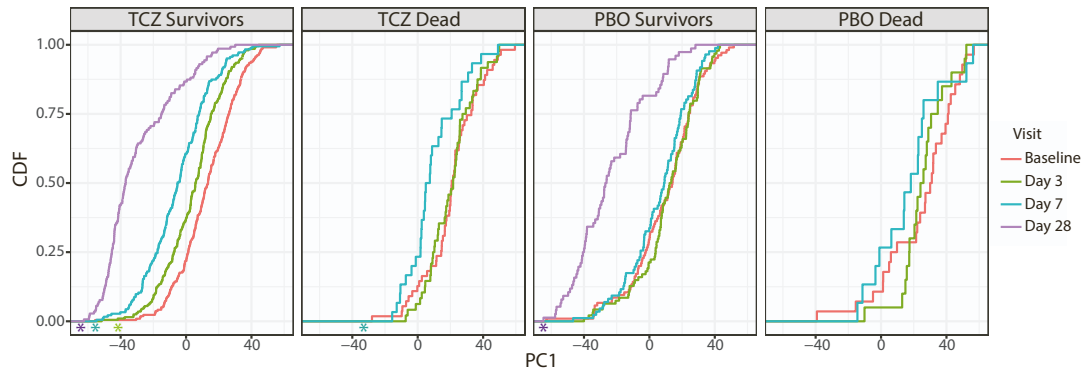


**Figure S6. Related to Figure 4. PCA analysis evaluating the benefit of tocilizumab treatment. (A)**

PCA (top) and density plots (bottom) showing longitudinal changes in serum protein signal measured by Olink for tocilizumab-treated and placebo samples collected at baseline, day 3, day 7, day 28 and healthy controls. **(B)** Cumulative distribution function plot showing distribution of Olink data across indicated Olink treatment groups. \*Indicates  $P$  value  $<0.05$  from Kolmogorov-Smirnov test performed between the indicated timepoints relative to baseline. **(C)** Cumulative distribution function plot showing distribution of indicated RNA-seq treatment groups. \*Indicates  $P$  value  $<0.05$  from Kolmogorov-Smirnov test performed between the indicated timepoints relative to baseline.

CDF, cumulative distribution function; CTRL, control; PBO, placebo; PCA, principal component analysis; TCZ, tocilizumab.

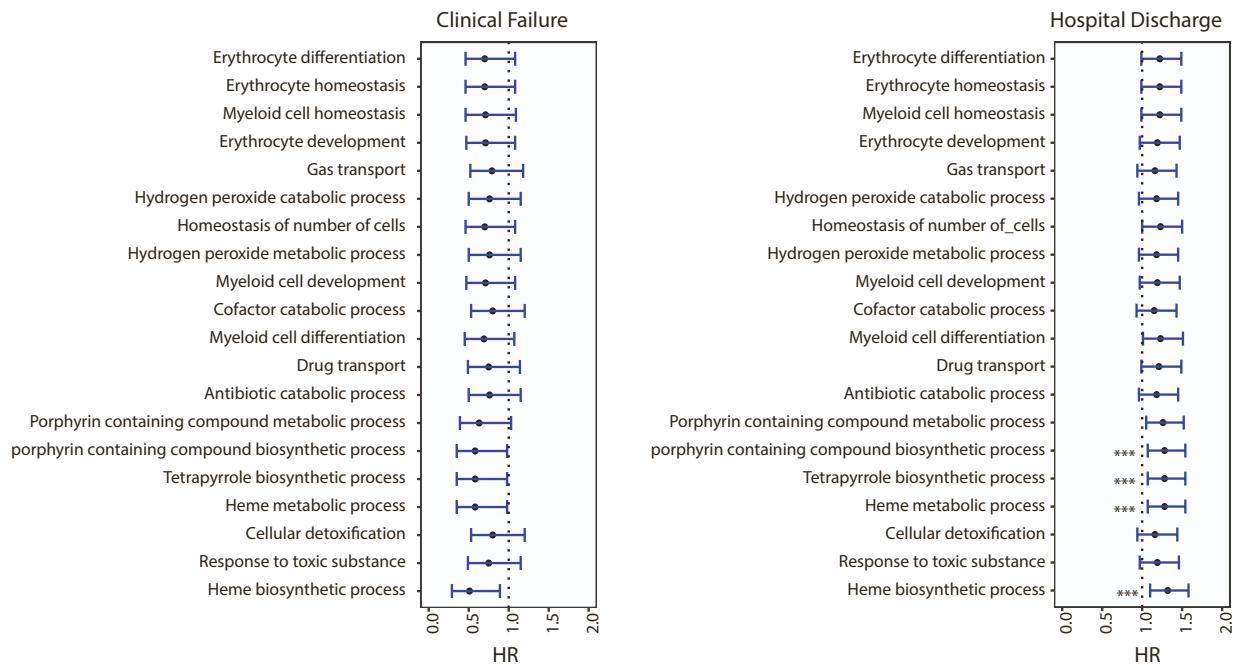


**Figure S7. Related to Figure 5. Tocilizumab treatment leads to upregulation of genes prognostic for**

**better clinical outcomes.** Forest plot showing hazard ratios with 95% confidence intervals identified using Cox proportional hazard model depicting clinical failure (left) from COVID19 and time to hospital

discharge (right) for pathways shown in Figure 5D. \*\*\*Represents Benjamini-Hochberg adjusted *P* value <0.05. Only patients with moderate severity (Baseline severity score < 4) were included for the analysis.

HR, hazard ratio.

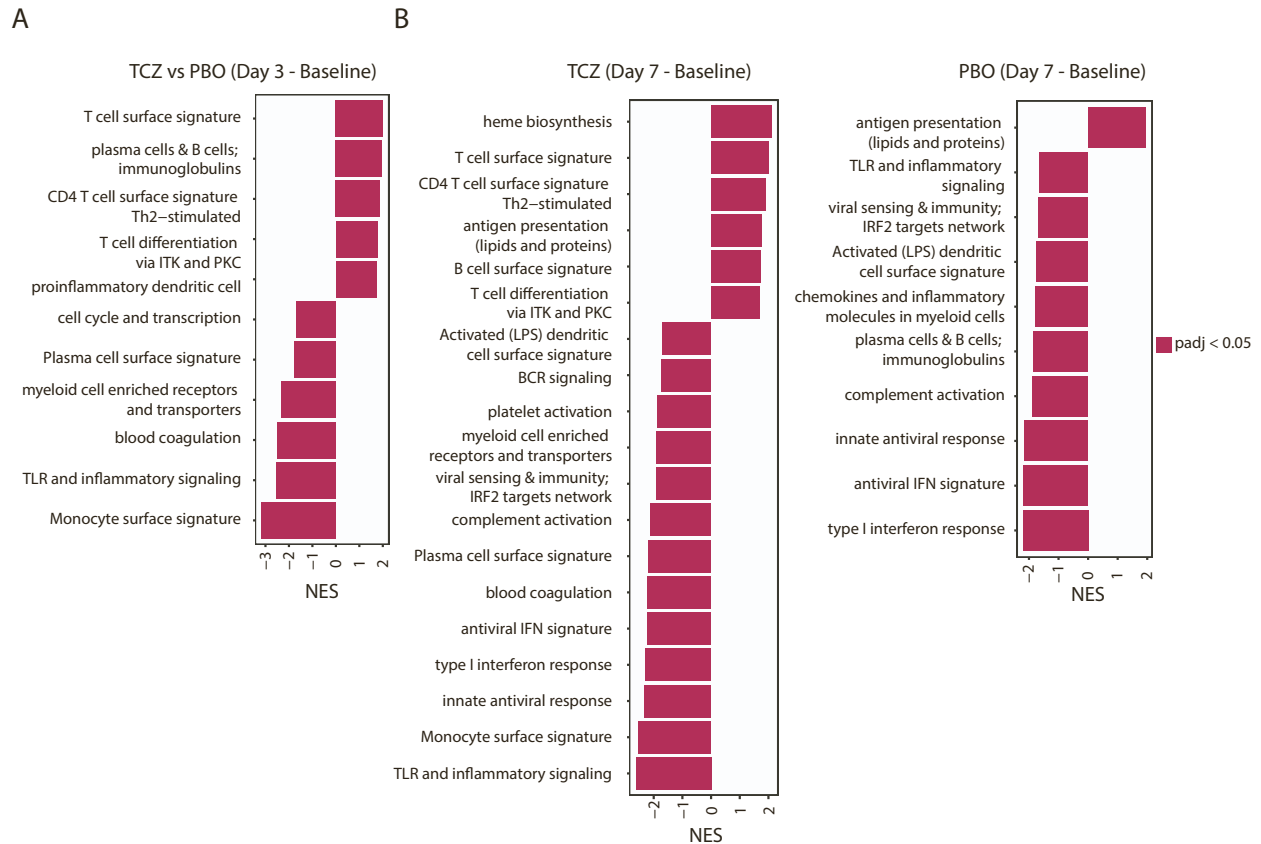


**Figure S8. Related to Figure 6. Effect of tocilizumab treatment on immune pathways. (A)** Bar plot showing immune pathways enriched among genes showing a greater response to tocilizumab compared to placebo by day 3 (calculated as [tocilizumab day 3 – tocilizumab day 1] – [placebo day 3 – placebo day 1]). **(B)** Bar plot showing FGSEA results for immune pathways enriched among genes responsive to tocilizumab and placebo by Day 7.

CD, cluster of differentiation; HLA, human leukocyte antigen; IFN, interferon; IRF, interferon regulatory factors; ITK, IL-2 inducible T cell kinase; LPS, lipopolysaccharide; NES, normalized enrichment score;

NK, natural killer; padj, adjusted *P* value; PKC, protein kinase C; PBO, placebo; TCZ, tocilizumab; Th, T helper cell; TLR, toll-like receptor.

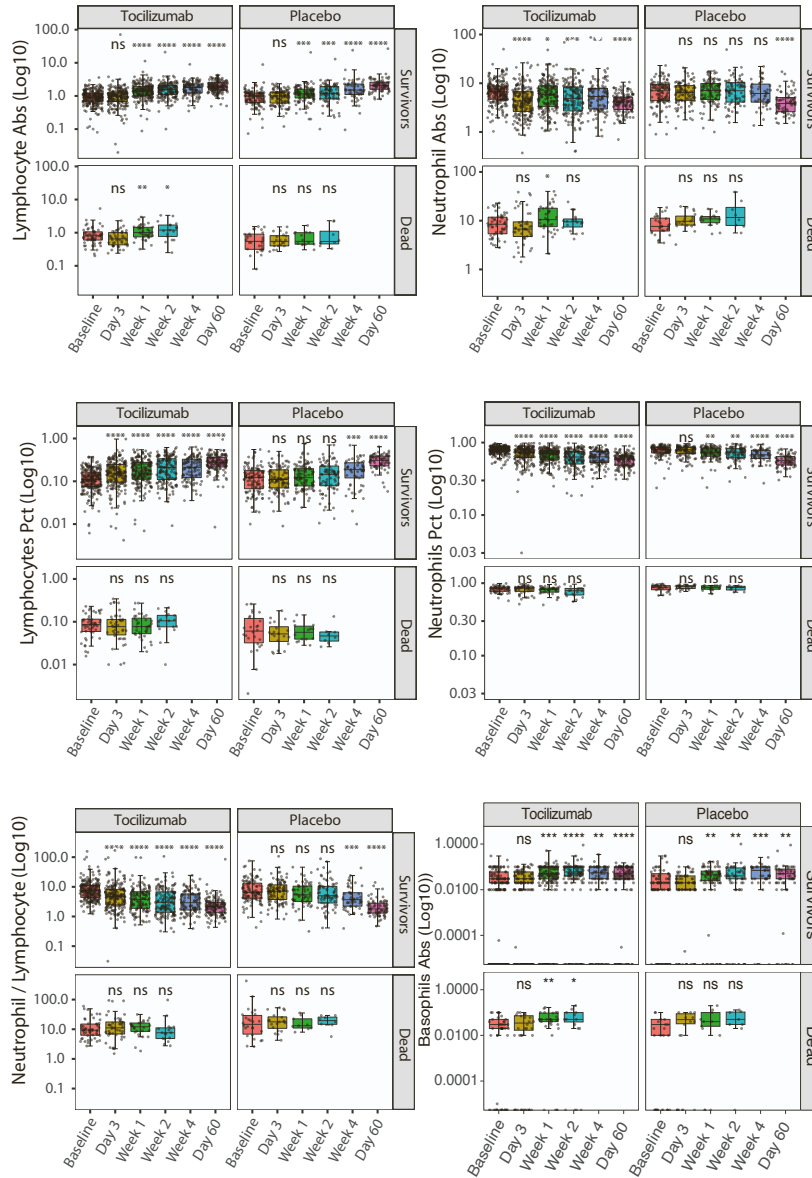
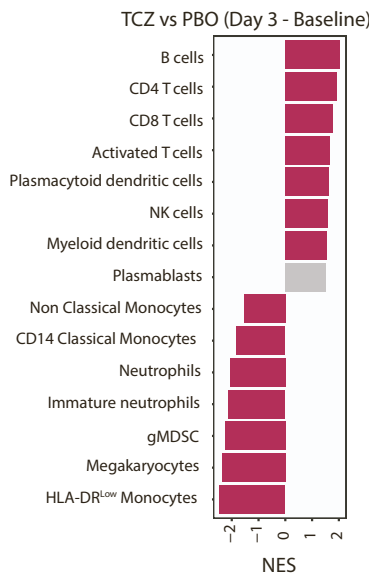


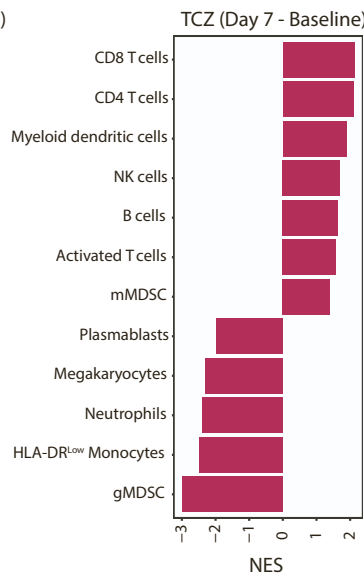
**Figure S9. Related to Figure 6. Effect of tocilizumab treatment on blood cell counts.** Boxplot showing eigengene expression of gene sets corresponding to blood cell types for patients treated with tocilizumab and placebo across timepoints. \*Represents statistical significance using pairwise T tests at each timepoint using baseline as reference the reference group. \*  $\leq 0.05$ , \*\*  $\leq 0.01$ , \*\*\*  $\leq 0.001$ , and \*\*\*\*  $\leq 0.0001$ . Number of patients per time point are indicated in Supplementary Table 5.

Abs, absolute; NS, not significant; Pct, percent.

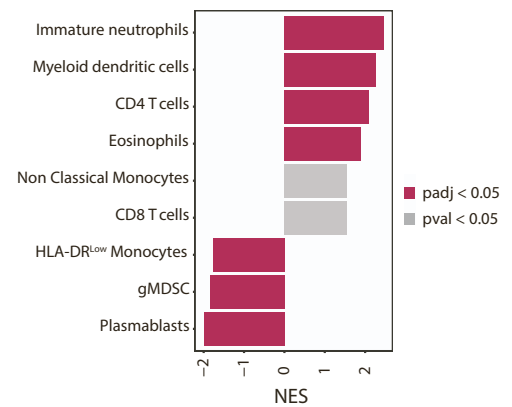
A



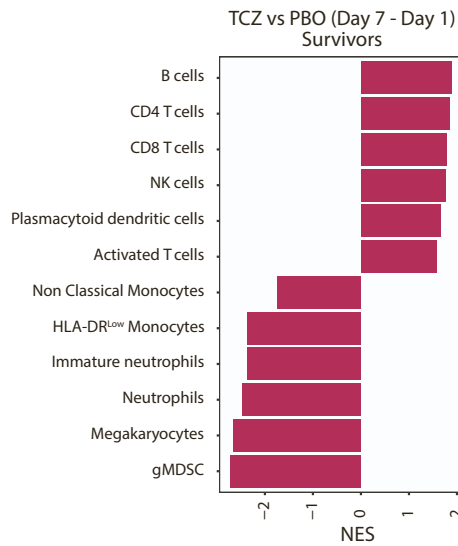
B



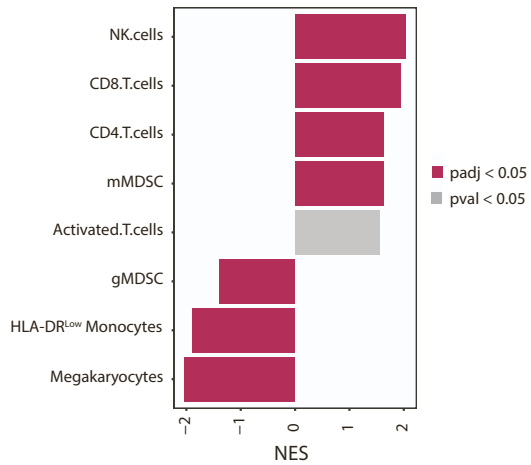
**PBO (Day 7 - Baseline)**



C



**TCZ vs PBO (Day 7 - Day 1) Dead**



D

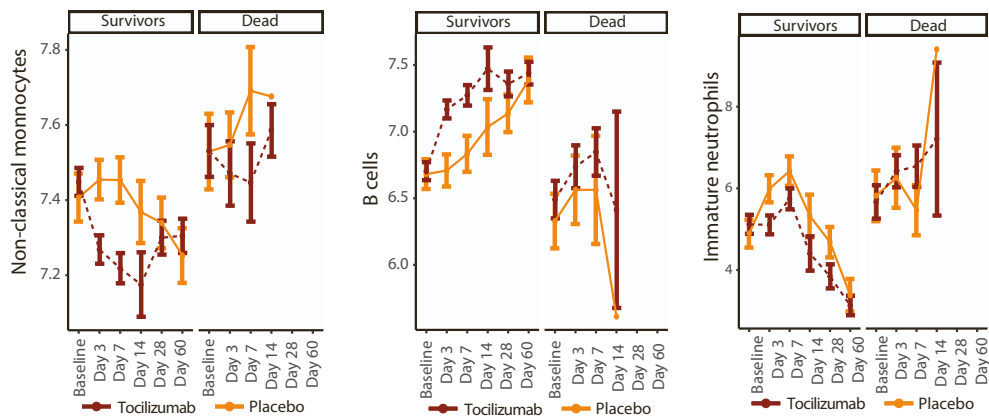


**Figure S10. Related to Figure 6. Effect of tocilizumab treatment on cell type signatures.** (A) Bar plot showing cell types enriched among genes showing a greater response to tocilizumab compared to placebo by day 3 (calculated as [tocilizumab day 3 – tocilizumab day 1] – [placebo day 3 – placebo day 1]). (B) Bar plots showing FGSEA results for blood cell types enriched among genes responsive to tocilizumab and placebo treatment by day 7. (C) Bar plot showing cell types enriched among genes showing a greater response to tocilizumab compared to placebo by day 7 (calculated as [tocilizumab day 7 – tocilizumab day 1] – [placebo day 7 – placebo day 1]) for survivors compared to those who died by day 28. (D) Line plots showing eigengene expression of gene sets corresponding to blood cell types for cases treated with tocilizumab and placebo across timepoints faceted by patients surviving and those dead by day 28.

CD, cluster of differentiation; gMDSC, granulocytic myeloid-derived suppressor cells; HLA, human leukocyte antigen; mMDSC, monocytic myeloid-derived suppressor cells; NES, normalized enrichment score; NK, natural killer; padj, adjusted P value; pval, P value; PBO, placebo; TCZ, tocilizumab.

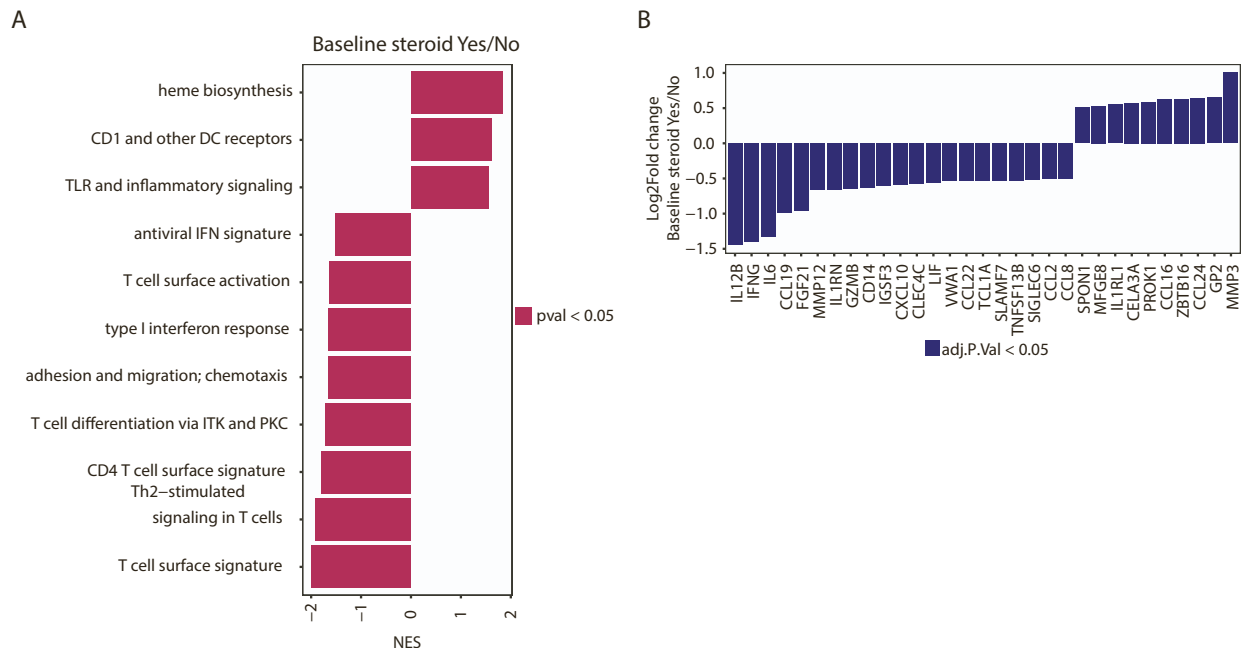


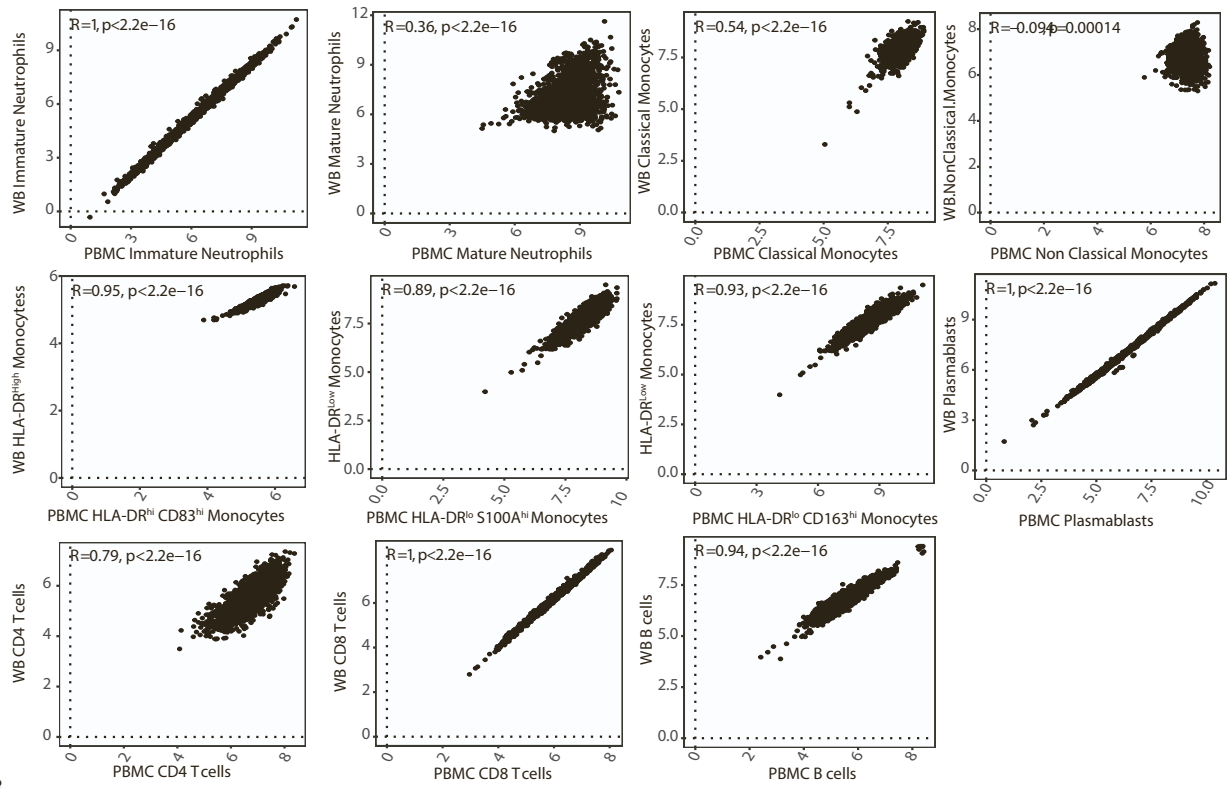
**Figure S11. Related to Figure 2 and 4. Effect of corticosteroid treatment on blood transcript and serum protein levels at baseline.** (A) Bar plot showing immune pathways enriched among genes

showing differential expression between subjects treated with (n = 93) or without corticosteroids (n = 316) sampled at baseline. **(B)** Column plot showing log<sub>2</sub>fold difference in the abundance (Y-axis) for the serum proteins significantly different at baseline between COVID19 subjects untreated (n = 304) or treated with corticosteroids (n = 84) at baseline.

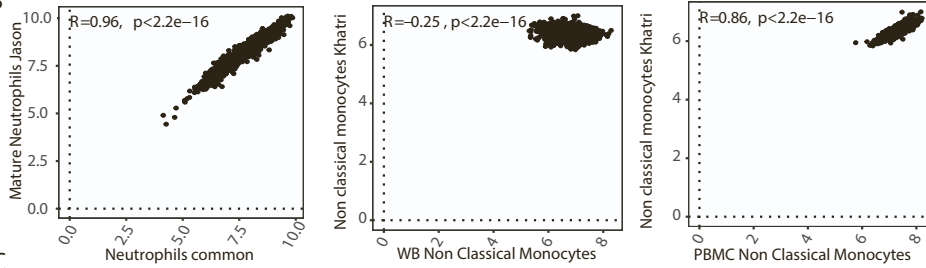
CD, cluster of differentiation; DC, dendritic cell; IFN, interferon; ITK, IL-2 inducible T cell kinase; NES, normalized enrichment score; PKC, protein kinase C; pval, *P* value; Th, T helper cell; TLR, toll-like receptor.



A



B



C

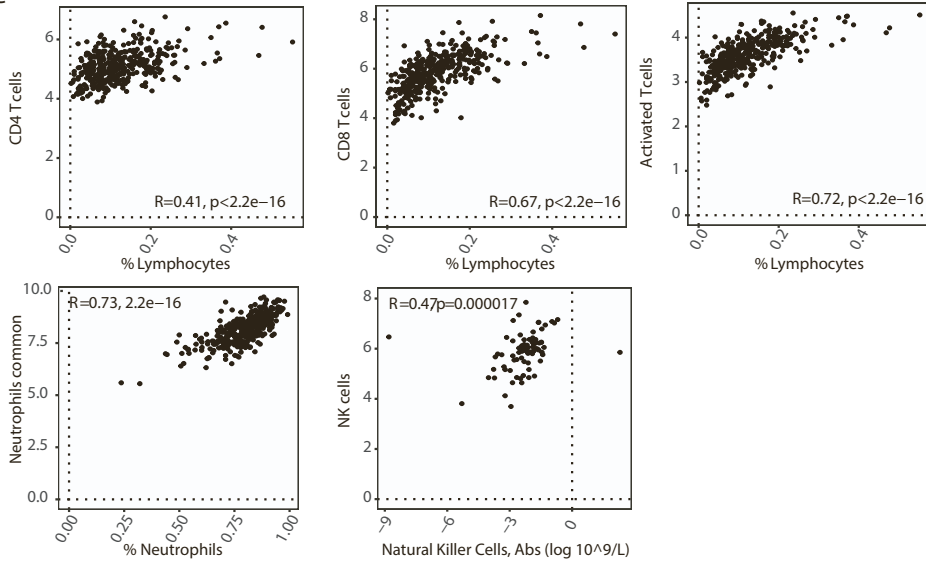


**Figure S12. Related to Figure 3 and 6. Quality assessment of blood cell type gene sets. (A)** Scatter plots showing correlation between the eigengene values of gene sets generated from pooled samples from whole blood and PBMCs (Y-axis) compared to the eigengene values from PBMCs. The cell types corresponding to the gene sets are indicated on the axis labels. **(B)** Scatter plots showing correlation between the eigengene values of mature neutrophils and nonclassical monocytes gene sets generated in this work (X-axis) compared to the eigengene values from published gene sets (Y-axis). The cell types corresponding to the gene sets are indicated on the axis labels. **(C)** Scatter plots showing correlation between the eigengene values of gene sets derived in this study (X-axis) compared to clinical hematology-based blood cell frequency. The cell types corresponding to the gene sets are indicated on axis labels.

CD4, cluster of differentiation 4; HLA, human leukocyte antigen; NK, natural killer; PBMC, peripheral blood mononuclear cell; WB, whole blood.

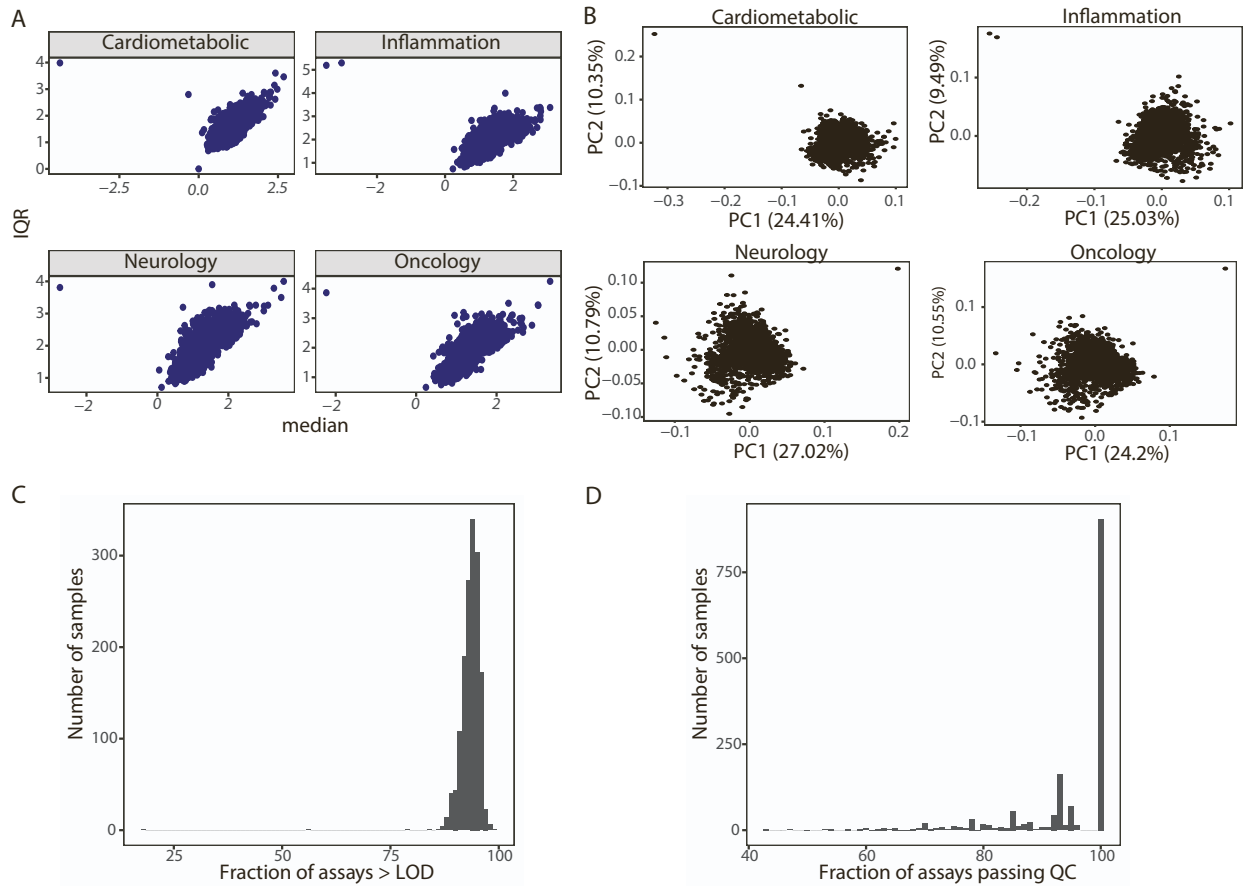


**Figure S13. Related to Figure 2 and 4. Quality assessment of Olink data. (A)** Scatter plot between interquartile range and median calculated across all samples for 1472 proteins split by the representative panels. **(B)** PCA analysis plotting PC1 and PC2 for 4 Olink panels where each point represents a sample. **(C)** Histogram plot wherein the x-axis represents the fraction of assays per sample with NPX values above LOD. Y-axis represents the number of samples. Two samples are highlighted where the fraction of assays with NPX above LOD were <75%. These were removed from downstream analysis. **(D)** Histogram plot wherein the x-axis represents the fraction of assays per sample that pass Olink's internal QC. Y-axis represents the number of samples. 86 samples are highlighted where the fraction of assays that pass QC were <75%. These were removed from downstream analysis. LOD, limit of detection; PCA, principal component analysis; QC, quality control.